CHEMISTRY
A EUROPEAN JOURNAL

DOI: 10.1002/chem.200501051

Enzyme-Free Amperometric Sensing of Glucose by Using Gold Nanoparticles

Bikash Kumar Jena and C. Retna Raj*[a]

Abstract: A nonenzymatic electrochemical method is described for the detection of glucose by using gold (Au) nanoparticles self-assembled on a three-dimensional (3D) silicate network obtained by using sol–gel processes. The nanosized Au particles have been self-assembled on the thiol tail groups of the silicate network and enlarged by hydroxylamine. The Au nanoparticles efficiently catalyze the oxidation of glucose at less-positive potential (0.16 V) in phosphate buffer solution (pH 9.2) in the absence of any enzymes or redox mediators. The Au nanoparticle-modified transducer (MPTS-nAuE) was successfully used for the amperometric sensing of glucose and it showed excellent sensitivity with a detection limit of 50 nM. The common interfering agent ascorbate (AA) does not interfere with the detection of glucose. The MPTS-nAuE transducer showed individual voltammetric responses for glucose and AA. This transducer responded linearly to glucose in the range of 0–8 mM and the sensitivity of the transducer was found to be 0.179 $nA\,cm^{-2}\,nM^{-1}$. Excellent reproducibility, and long-term storage and operational stability was observed for this transducer.

Keywords: analytical methods · electrochemistry · gold · nanotechnology · sensors

Introduction

The development of sensing devices for the fast and reliable monitoring of glucose and the carbohydrates for the treatment and control of diabetes has been a focal subject in analytical chemistry for the past few decades.[1] Optical methods have been commonly used for the indirect detection of carbohydrates,[2–4] however, the sensitivity and selectivity of these methods are low[4] and they involve the enzyme glucose oxidase/glucose dehydrogenase, or require special reagents for derivatization.[2–4] Electrochemical methods have been the subject of considerable interest[5–9] because a low detection limit can be achieved easily. Most of the electrochemical methods are based on the use of the enzyme glucose oxidase that specifically catalyzes the oxidation of glucose to glucolactone.[5,6] The electrochemical biosensing of glucose is either based on the redox reaction of mediators that are attached onto the electrode surface along with the enzyme or based on the electrochemical oxidation of enzymatically generated H_2O_2.[5,6] In the former case, the internally wired redox mediators electrochemically access the flavin cofactor of glucose oxidase, whereas the latter case involves the reduction of oxygen to hydrogen peroxide by the enzyme glucose oxidase. Despite the fact that the enzyme-based sensors show high-selectivity and excellent sensitivity: 1) they suffer from the lack of stability due to the intrinsic nature of the enzymes, 2) the oxidation of enzymatically generated H_2O_2 requires a high overpotential and is prone to interference due to other redox-active molecules such as AA. Various other approaches have been used to circumvent these difficulties by using different electrodes.[7–9] The noble metals Pt and Au have been widely used for the oxidation of glucose.[7e,f,8,9] It is well known that the Pt electrode rapidly loses its activity due to poisoning by the reaction intermediate. Very recently, the Pt-nanotubule and macroporous Pt-modified electrodes have been shown to exhibit good sensitivity towards glucose.[7e,f] However, these electrodes require electrochemical cleaning before each measurement to renew the electrode surface. The pulse amperometric (PA) method uses a Au working electrode offering excellent sensitivity compared to the other methods.[8] This PA method requires pulse-generation circuits that are relatively expensive and a high potential needs to be applied during the pulse process in order to avoid the fouling of

[a] B. K. Jena, Dr. C. R. Raj
Department of Chemistry, Indian Institute of Technology
Kharagpur 721 302 (India)
Fax: (+91) 3222-282-252
E-mail: crraj@chem.iitkgp.ernet.in

Supporting information for this article is available on the WWW under http://www.chemeurj.org/ or from the author.

electrode surface. The electrode surface is gradually etched during the pulse process because of the high potential. Therefore it is desirable to develop a stable interference-free nonenzymatic electrochemical sensor for the sensing of glucose.

In recent years increasing efforts have been devoted to investigating the optical and electrochemical properties of nanomaterials.[10–12] The Au nanoparticles have been widely used for optical and electrochemical applications.[11,12] Although bulk Au metal is a poor catalyst, recent studies show that nanosized Au particles exhibit extraordinary catalytic activity.[13–15] The large surface-to-volume ratio and interface-dominated properties that differ from those of the bulk counterparts are considered as the driving force in nanoparticle-assisted catalysis.[14]

Sol–gel technology provides a versatile way to prepare a three-dimensional (3D) silicate network through the hydrolysis and condensation of silicon alkoxide precursors.[16,17] The silicate network prepared through the sol–gel process is particularly attractive in the development of sensing devices, as the network exhibits tunable porosity, high thermal stability, and chemical inertness. The compound (3-mercaptopropyl)trimethoxysilane (MPTS) is known to form a 3D network with thiol tail groups by the hydrolysis and condensation process.[18] As the thiol groups are distributed throughout the network, the nanosized Au particles can be assembled both inside and on the surface of the network.

Our group is interested in the development of an electrochemical sensor for the detection of different biomolecules.[19] In an effort to develop an efficient enzyme-free method for the detection of glucose without interference, we have exploited Au nanoparticles self-assembled on the thiol groups of a 3D silicate network derived by using a sol–gel process. Herein we report the electrocatalytic detection of glucose by using Au nanoparticles in the absence of any enzymes or redox mediator.

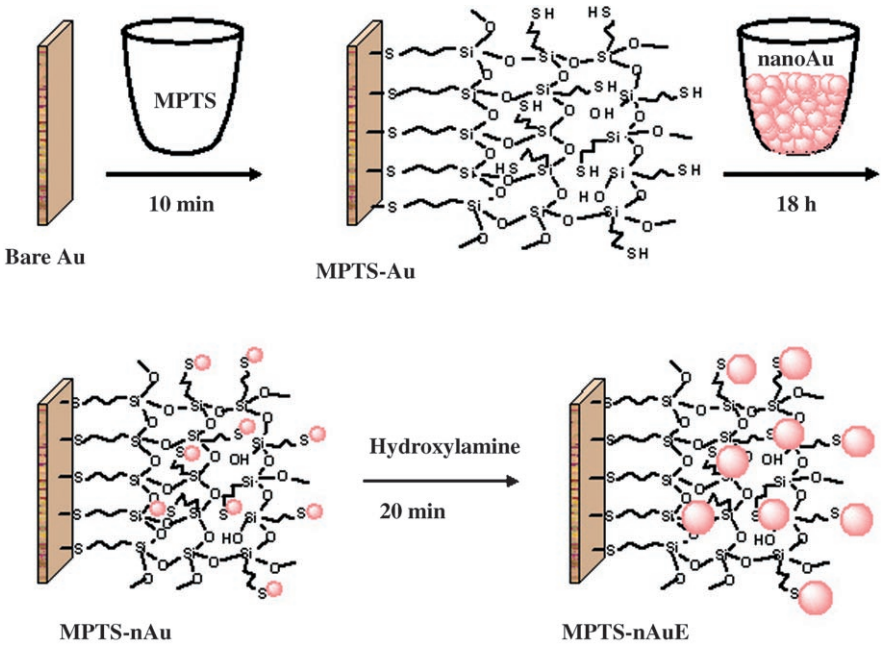

Scheme 1. Schematic representation for the fabrication of the Au nanoparticle-modified transducer.

Results and Discussion

Characterization of the nanoparticle self-assembled transducer: The Au nanoparticles were self-assembled on the thiol groups of the silicate network according to Scheme 1. At first, the MPTS was self-assembled on a polycrystalline Au electrode, and then the Au nanoparticles were chemisorbed onto the thiol groups present inside and on the surface of the silicate network. Figure 1 represents the voltammetric response of the MPTS-modified Au electrode before and after the self-assembling of Au particles towards the redox marker $K_3Fe(CN)_6$. As shown in Figure 1, the MPTS-modified electrode shows sluggish electron-transfer kinetics for $K_3Fe(CN)_6$ with a peak-to-peak separation (ΔE_p) of more than 200 mV due to the kinetic hindrance exerted by the silicate network, whereas the same electrode displays facile electron-transfer kinetics with a ΔE_p value of around 65 mV after the self-assembling of Au nanoparticles. The facilitated electron-transfer reaction is ascribed to the presence of Au nanoparticles on the thiol groups of the silicate network.

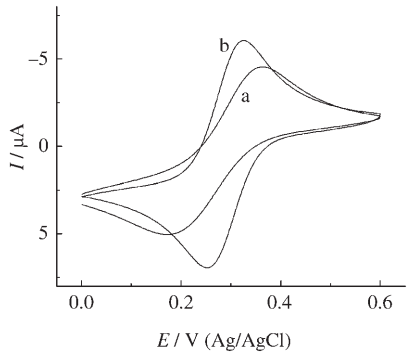

Figure 1. Cyclic voltammetric response of the MPTS-modified polycrystalline Au electrode: a) before and; b) after the self-assembling of Au nanoparticles toward the redox marker $K_3Fe(CN)_6$ (1 mM) in 0.1 M KCl. Scan rate: 100 mV s^{-1}.

Figure 2 displays the cyclic voltammograms obtained for the Au nanoparticles self-assembled on the silicate network

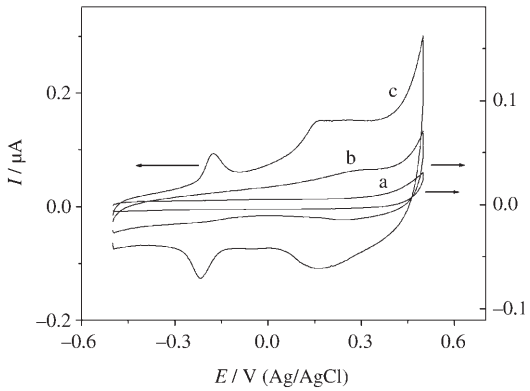

Figure 2. Cyclic voltammograms obtained for: a) MPTS-modified polycrystalline Au electrode; b) MPTS-nAu; c) MPTS-nAuE electrodes in 0.1 M PBS. Scan rate: 10 mV s^{-1}.

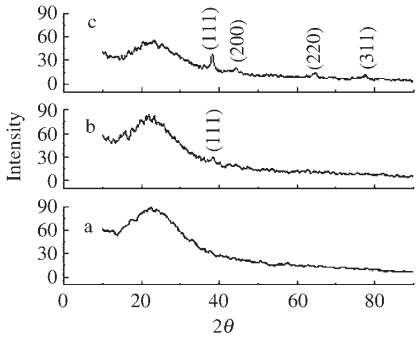

Figure 3. XRD patterns obtained for: a) MPTS-modified glass slide; b) MPTS-nAu; c) MPTS-nAuE glass slides.

before (MPTS-nAu) and after enlargement (MPTS-nAuE). The MPTS-nAu electrode shows a voltammetric peak at around +0.24 V, whereas the MPTS-nAuE electrode shows two peaks at $+0.155 \pm 0.010$ and -0.175 ± 0.010 V. The appearance of two voltammetric peaks for the MPTS-nAuE electrode suggests that enlargement of the Au nanoparticles by hydroxylamine influences the surface morphology. The voltammetric features observed for the MPTS-nAuE electrodes are similar to those of the Au (111) single-crystal electrode, indicating that self-assembled nanoparticles have a Au (111) face. The Au (111) electrode shows two voltammetric peaks at +0.2 and −0.2 V (SCE) in phosphate buffer solution (PBS) and were ascribed to the formation of surface oxides.[9b,22] In the present investigation, the voltammetric peaks observed for the MPTS-nAu and MPTS-nAuE electrodes are ascribed to the formation of incipient hydrous oxides AuOH by the process of premonolayer oxidation. Such a voltammetric response has not been observed either at the MPTS-modified Au electrode or unmodified polycrystalline Au electrode, suggesting that the voltammetric features of MPTS-nAu and MPTS-nAuE electrodes are due to the presence of Au nanoparticles. The existence of a Au (111) face at the nanoparticles self-assembled on the silicate network has been examined by measuring the XRD pattern. The XRD pattern obtained for the self-assembled nanoparticles before enlargement shows a less intense peak corresponding to the (111) plane of a face-centered cubic lattice of gold (Figure 3). On the other hand, the XRD pattern obtained after the enlargement of particles shows four peaks corresponding to the (111), (200), (220), and (311) planes. As shown in Figure 3, although four peaks for different orientations have been observed after enlargement, the peak corresponding to the (111) plane is intense, demonstrating that (111) plane is the predominant orientation. The XRD pattern supports the voltammetric features observed for the MPTS-nAu and MPTS-nAuE electrodes.

The size of the nanoparticles before and after enlargement was calculated from the XRD pattern by using the Scherrer equation.[20] The size of the particles before and after enlargement was found to be 14 and 33 nm, respectively. The atomic force microscopy (AFM) measurement (see Supporting Information) shows that the enlargement of the particle by hydroxylamine results in the formation of nanoislands and the particles were found to have an average size of 35 nm, in good agreement with the value obtained from the XRD measurement. The absorption spectra (see Supporting Information) obtained for the Au nanoparticles self-assembled on an MPTS-modified glass slide shows a plasmon absorption band at 522 nm. The enlargement of the particles by hydroxylamine increases the absorbance substantially and shifts (see Supporting Information) the λ_{max} to a higher wavelength ($\lambda_{max} = 536$ nm, peakwidth-at-half-maximum = 136 nm) suggesting a particle size of about 35 nm.[21] The surface area of the Au particles self-assembled on the silicate network before and after enlargement has been determined by chronoamperometry and a 3.6-fold increase in the surface area was observed after enlargement.

Electrocatalytic oxidation of glucose: Figure 4 compares the voltammograms obtained for the oxidation of glucose at the MPTS-modified polycrystalline Au electrode, and the MPTS-nAu and MPTS-nAuE electrodes. The MPTS-modified polycrystalline Au electrode does not show any charac-

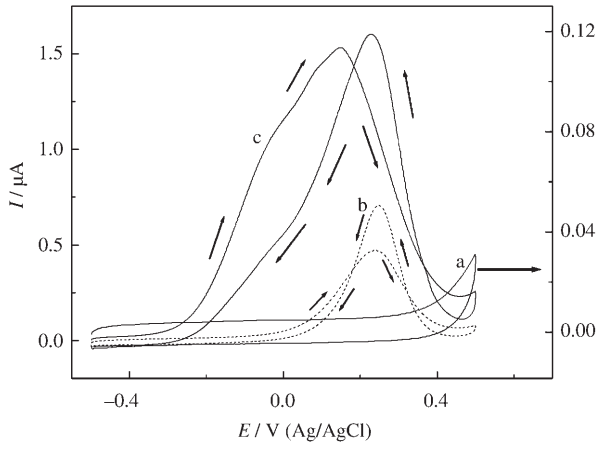

Figure 4. Cyclic voltammograms for the oxidation of glucose (1 mM) at: a) MPTS-modified polycrystalline Au electrode; b) MPTS-nAu electrode; c) MPTS-nAuE electrode in 0.1 M PBS. Scan rate: 10 mV s^{-1}.

teristic response (Figure 4a) for the oxidation of glucose. However, the nanoparticle self-assembled electrodes exhibit a typical voltammetric response for glucose. The MPTS-nAu electrode shows a well-defined voltammetric peak at 0.24 V whereas the MPTS-nAuE electrode shows the oxidation peak at much less-positive potential (~0.16 V). These results show that the Au nanoparticles on the silicate network efficiently catalyze the oxidation process. Interestingly, the hydroxylamine enlargement of the particle results in a threefold increase in the peak current (forward scan) for the oxidation of glucose. The close examination of the voltammetric features obtained for the oxidation of glucose at the MPTS-nAu and MPTS-nAuE electrodes reveals interesting results. Both electrodes (MPTS-nAu and MPTS-nAuE) display anodic current for glucose during the reverse sweep. At the MPTS-nAu electrode the oxidation potential in the forward and reverse scans remained the same (0.24 V) and the peak current observed in the reverse scan was much higher than that in the forward scan. On the other hand, at the MPTS-nAuE electrode, the oxidation potential in the forward scan was less positive (~0.16 V) than that of the reverse scan; the magnitude of peak current in the reverse scan was slightly higher than that of the forward scan. The MPTS-nAuE electrode shows an additional broad prepeak at around −0.06 V. It should be pointed out here that such a prepeak was observed only at higher concentrations of glucose ($\geq$1 mM) and was not observed in the micromolar range. The MPTS-nAu electrode did not show such a prepeak either at low or higher concentration. These results indicate that the glucose oxidation is very sensitive to the particle size and surface orientation; the XRD pattern for MPTS-nAu shows only one less-intense peak corresponding to the Au (111) orientation whereas MPTS-nAuE shows four peaks corresponding to different planes with predominant (111) orientation (vide supra). It is worthwhile to mention here that the onset potential for the oxidation of glucose at the MPTS-nAuE electrode is much more negative (<-0.3 V), indicating that the self-assembled Au nanoparticles function as an excellent electrocatalyst. The enlargement of the particles increases the surface area and the high surface area of the MPTS-nAuE electrode effectively increases its catalytic activity towards the oxidation of glucose. The catalytic effect of the Au nanoparticles can be rationalized by considering the incipient hydrous oxide/adatom mediator model.[9b,22] The Au nanoparticles undergo oxidation at unusually low potential, resulting in the formation of incipient hydrous oxides and they function like a potential mediator and efficiently catalyze the oxidation of glucose.

The main objective of the present investigation was to develop a stable enzyme-free sensor for the detection of glucose at low concentration without any interference from other electroactive interfering agents like AA. Since the MPTS-nAuE electrode efficiently catalyzes the oxidation of glucose, it has been used for the detection of glucose at low concentration. As shown in the Figure 5 the MPTS-nAuE electrode is very sensitive to the addition of glucose and the peak current at about 0.16 V gradually increases with the concentration of glucose. Here it is worth pointing out that the cathodic peak current at about 0.15 V gradually decreases upon each addition of glucose. This is consistent with the strong catalytic effect of the Au nanoparticles on the silicate network and the participation of surface oxide in the catalysis. The anodic and cathodic peak observed in the negative potential region disappeared upon the addition of glucose.

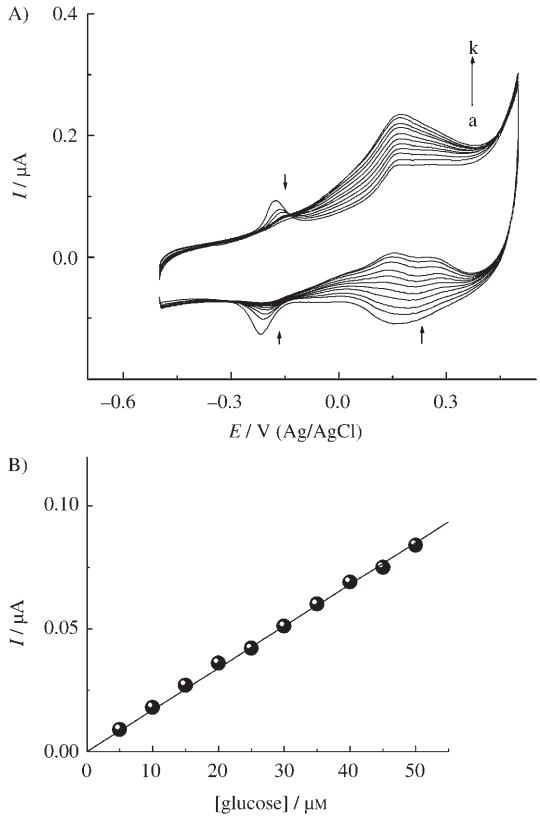

Figure 5. A) Cyclic voltammograms for the oxidation of glucose at the MPTS-nAuE electrode in 0.1 M PBS at different concentrations. Each addition increased the concentration by 5 μM. Scan rate: 10 mV s^{-1}. B) Corresponding calibration plot.

Amperometric sensing of glucose: For practical application of any sensor, it is desirable to use constant potential amperometry that is a method that can evaluate the performance of the transducer. In the present investigation, the performance of the MPTS-nAuE transducer towards the detection of glucose has been tested by recording the amperometric response (Figure 6). The potential of the electrode was held at 0.16 V and glucose was injected at regular intervals. We noted a rapid increase in the current after each addition of glucose (75 nM) to the stirred supporting electrolyte solution. The peak current linearly ($R^2=0.9988$) increased with the concentration and the sensitivity was calculated to be 0.179 nA cm^{-2} nM^{-1}. The MPTS-nAuE electrode could detect glucose concentrations as low as 50 nM and the amperometric response was very stable. As the normal physiological level of glucose is 3–8 mM, the amperometric response of the present transducer at higher concentration was further

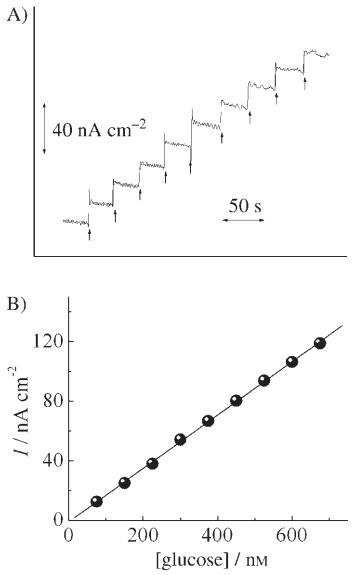

Figure 6. A) Amperometric current versus time (i–t) curve for the detection of glucose at the MPTS-nAuE electrode. Glucose (75 nM) was injected into the stirred 0.1 M PBS at regular intervals; arrows indicate the glucose injection. The potential of the electrode was held at 0.16 V. B) Corresponding calibration plot.

tested (Figure 7). As can be readily seen the transducer shows a linear response for a wide range of concentrations of glucose (0–8 mM), demonstrating the potential usefulness of the transducer.

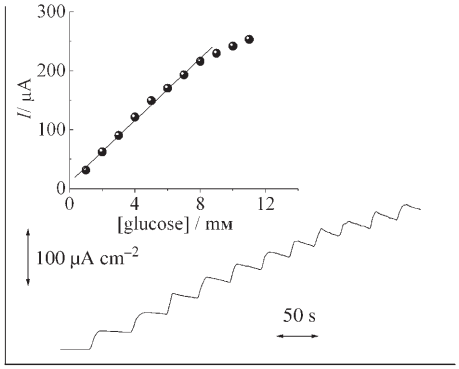

Figure 7. Amperometric current versus time (i–t) curve for the detection of glucose at the MPTS-nAuE electrode. Glucose (1 mM) was injected into the stirred 0.1 M PBS at regular intervals; all other conditions are similar to those from Figure 6. Inset shows the corresponding calibration plot.

Interference: As mentioned in the Introduction, the elimination of interferences due to easily oxidizable compounds present in the physiological system is a real challenge in the voltammetric detection of glucose. AA is one of the major interfering agents in the physiological system and this interference has to be eliminated in order to get accurate measurement of glucose. This interference can be eliminated by using a negatively charged polymer like Nafion or enzyme ascorbate oxidase that oxidizes AA to dehydroascorbic acid in the presence of oxygen. However, the immobilization of enzyme on the electrode surface is a difficult task, requiring a coupling agent or polymers that would decrease the sensitivity of the electrode towards glucose. In the present investigation, the MPTS-nAuE electrode has been successfully used for the detection of glucose without the interference from AA in the absence of enzyme or polymers. The normal physiological level of glucose at 3–8 mM is much higher than that of AA (~0.1 mM)). Therefore the selectivity towards glucose for the present electrode was tested in the presence of 0.1 mM AA. As shown in Figure 8, the MPTS-

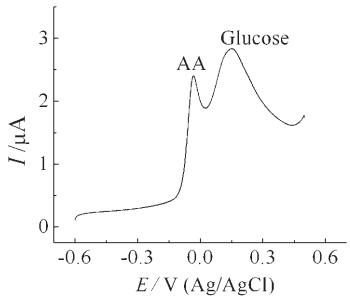

Figure 8. Linear-sweep voltammograms for the oxidation of glucose (0.1 mM) in the presence of AA (0.1 mM) in 0.1 M PBS. Scan rate: 100 mV s^{-1}.

nAuE electrode exhibits individual voltammetric peaks for AA and glucose. The presence of AA does not interfere with the voltammetric response of glucose; the sensitivity of the electrode in the presence and absence of AA does not change appreciably demonstrating that the present electrode can be successfully used for the individual or the simultaneous detection of glucose and AA.

Stability: The long-term storage and operational stability of the electrode is essential for the continuous monitoring of glucose. The stability of the present electrode was examined by using the same MPTS-nAuE electrode for 20 repetitive measurements in a supporting electrolyte solution containing 0.1 M glucose. The electrode used in this measurement was kept in 0.1 M PBS and was subjected to another 20 repetitive measurements after 24 h. Interestingly, we noticed no observable change in the peak potential and peak current for the oxidation of glucose in both sets of experiments. The coefficient of variation was calculated separately for the two sets of experiments and we found that it remained the same (0.36 and 0.37 %) in both sets. This shows that the electrode is stable and does not undergo poisoning by the oxidation product, and can be used for the repeated measurement of glucose. To further ascertain the operational stability of the present electrode, voltammetric measurement in a supporting electrolyte solution containing 0.1 M glucose was performed with the MPTS-nAuE electrode and the peak current for the oxidation of glucose was measured at regular intervals (every 4–5 hr) over a period of 26 h. As shown in Figure 9, the magnitude of the peak current did not change

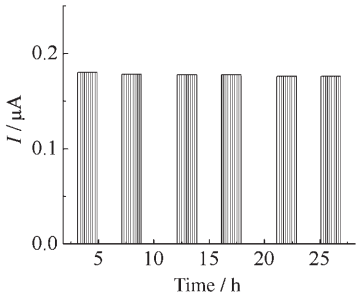

Figure 9. Plot of current versus time for the oxidation of glucose (0.1 mM) at the MPTS-nAuE electrode in 0.1 M PBS demonstrating the operational stability of the electrode.

appreciably during the whole set of experiments (26 hr), demonstrating that the MPTS-nAuE electrode is very stable and retains its sensitivity throughout the experiments. The long-term storage stability was tested by measuring the electrode response for a period of one week (see Supporting Information). The MPTS-nAuE electrode is robust; the response did not change appreciably in the first five days and we noted only 10% loss of activity after a storage time of one week in PBS at room temperature, demonstrating the long-term storage and operational stability. To check the reproducibility of the results, four different MPTS-nAuE electrodes were used for the voltammetric measurement of a solution containing 0.1 mM glucose. All the four electrodes exhibited identical voltammograms for the oxidation of glucose, confirming that the results are highly reproducible.

Conclusion

We have demonstrated for the first time that Au nanoparticles self-assembled on a silicate network efficiently catalyze the oxidation of glucose in the absence of any enzymes and redox mediators. Thanks to Au nanoparticles, the MPTS-nAuE transducer successfully detects glucose at a nanomolar level without any interference from the common interfering agent AA. The MPTS-nAuE transducer shows individual voltammetric peaks for glucose and AA, favoring the individual or simultaneous detection of both the analytes. The long-term storage and operational stability of the transducer has been successfully demonstrated. The major advantage of the present transducer is that it is highly sensitive for the detection of glucose at the nanomolar level and is very stable. Cleaning of the transducer before each measurement is not required. Further studies on the kinetics and mechanistic aspects are in progress.

Experimental Section

Materials: 3-(Mercaptopropyl)trimethoxysilane (MPTS) and $HAuCl_4$ were obtained from Aldrich and were used as received. All other chemicals used in this investigation unless mentioned otherwise were of Analar grade. All the solutions were prepared with Millipore water.

Instrumentation: Electrochemical measurements were performed by using a two-compartment three-electrode cell with a polycrystalline Au working electrode, a Pt-wire auxiliary electrode, and an Ag/AgCl (3 M NaCl) reference electrode. Cyclic voltammograms were recorded using a computer-controlled CHI643B electrochemical analyzer. X-ray diffraction analysis of self-assembled Au nanoparticles before and after enlargement was carried out with a Phillips X′pert PRO X-ray diffraction unit using Ni-filtered $Cu_{K\alpha}$ ($\lambda = 1.54$ Å) radiation. The crystallite size of the Au nanoparticles was determined by using the Scherrer formula.[20] AFM measurements were performed with a Nanonics SPM 100 system having a resolution of 300 dpi. The images were acquired in the tapping mode and the measurements were made with the quartz cantilever in air at room temperature. The force constant of the cantilever was 0.1–0.6 $N m^{-1}$ with a scan rate of 1–2 Hz. The UV-visible spectral measurements were performed with a Shimadzu UV-visible spectrophotometer (UV-1601).

Procedure: All glassware used in the preparation of colloidal Au nanoparticles was cleaned with freshly prepared aqua regia and was rinsed thoroughly with water. Citrate-stabilized Au nanoparticles of about 2.6 nm diameter were prepared by adding trisodium citrate (0.64 mL, 1.15%) and freshly prepared $NaBH_4$ (0.32 mL, 0.08%) in 1% trisodium citrate to water (30 mL) containing 1% $HAuCl_4$ (0.32 mL) and stirring the solution for 10 min at room temperature. The citrate-stabilized Au nanoparticles displayed a plasmon absorption band at 518 nm (see Supporting Information). The MPTS sol was prepared by dissolving MPTS, methanol, and water (as 0.1 M) in the molar ratio of 1:3:3 and stirring the mixture vigorously for 30 min. The MPTS sol existed as a 3D silicate network with free thiol groups due to the hydrolysis and condensation. The polycrystalline Au electrode of area 0.02 cm^2 was polished repeatedly with alumina (0.06 μm) and was sonicated in water for 15 min. The well-polished electrode was then subjected to electrochemical pretreatment by cycling the potential between −0.2 and +1.5 V in H_2SO_4 (0.25 M) at the scan rate of 10 $V s^{-1}$ for about 10 min or until a voltammogram with characteristics of a clean polycrystalline Au electrode was obtained. The electrochemically cleaned electrode was soaked in MPTS sol (0.5 mL) for 10 min. The MPTS self-assembled on the polycrystalline Au electrode and existed as a 3D silicate network full of thiol tail groups (Scheme 1). The MPTS-modified electrode was then soaked in a solution containing colloidal Au nanoparticles for 18 h. The Au nanoparticles chemisorbed on the thiol tail groups of the 3D silicate network. The enlargement of the Au nanoparticles self-assembled on the silicate network was carried out by using hydroxylamine according to the literature procedure[23] with little modification. Typically, the nanoparticle self-assembled electrode was soaked in a solution containing NH_2OH (0.3 mM) and $AuCl_4^-$ (0.3 mM) with constant shaking for 20 min. Hereafter the nanoparticle self-assembled electrodes before and after enlargement are referred to as MPTS-nAu and MPTS-nAuE, respectively. These electrodes were rinsed repeatedly with water and kept in PBS before subjecting to electrochemical experiments. For XRD, AFM, and UV/Vis spectral measurements, the microscopic glass slide or coverslip was cleaned well with acetone and water and was soaked in a methanolic solution of MPTS for about 18 h. The MPTS-modified glass slide or coverslip was washed with copious amounts of water and was then soaked in a solution containing colloidal Au nanoparticles for 5 h. The enlargement of Au nanoparticles self-assembled on the glass slide or coverslip was performed as mentioned earlier. All the electrochemical experiments were carried out in an argon atmosphere. PBS (0.1 M, pH 9.2) was used as a supporting electrolyte in all experiments. All the experiments were repeated at least three times and reproducible results were obtained.

Acknowledgements

This work was supported by grants from CSIR (No. 01(1895)/03/EMR-II) and DST (No. SR/FTP/CSA-15/2002). The authors are grateful to Professor Chacko Jacob of the Materials Science Center, Indian Institute of Technology, Kharagpur, for the AFM measurements.

[1] a) G. Reach, G. S. Wilson, *Anal. Chem.* **1992**, *64*, 381A–386A; b) A. P. F. Turner, B. Chen, A. P. Sergey, *Clin. Chem.* **1999**, *45*, 1596–1601.
[2] a) R. J. Russell, M. V. Pishko, C. C. Gefrides, M. J. McShane, G. L. Cote, *Anal. Chem.* **1999**, *71*, 3126–3132; b) T. D. James, H. Shinmori, S. Shinkai, *Chem. Commun.* **1997**, 71–72; c) N. DiCesare, J. R. Lakowicz, *Org. Lett.* **2001**, *3*, 3891–3893.
[3] a) D. B. Cordes, A. Miller, S. Gamsey, Z. Sharret, P. Thoniyot, R. Wessling, B. Sinaram, *Org. Biomol. Chem.* **2005**, *3*, 1708–1713; b) J. C. Pickup, F. Hussain, N. D. Evans, O. J. Rolinski, D. J. S. Birch, *Biosens. Bioelectron.* **2005**, *20*, 2555–2565; c) S. A. Asher, V. L. Alexeev, A. V. Goponenko, A. C. Sharma, I. K. Lednev, C. S. Wilcox, D. N. Finegold, *J. Am. Chem. Soc.* **2003**, *125*, 3322–3329.
[4] a) T. D. James, S. Shinkai in *Host–Guest Chemistry, Vol. 218*: *Artificial Receptors as Chemosensors for Carbohydrates*, Springer, Berlin, **2002**, p. 159; b) R. Badugu, J. R. Lakowicz, C. D. Geddes, *Anal. Chem.* **2004**, *76*, 610–618.
[5] a) G. S. Wilson, Y. Hu, *Chem. Rev.* **2000**, *100*, 2693–2704; b) A. Heller, *Acc. Chem. Res.* **1990**, *23*, 128–134.
[6] a) N. Mano, A. Heller, *Anal. Chem.* **2005**, *77*, 729–732; b) J.-M. Zen, A. S. Kumar, C.-R. Chung, *Anal. Chem.* **2003**, *75*, 2703–2709; c) F. Battaglini, P. N. Bartlett, J. H. Wang, *Anal. Chem.* **2000**, *72*, 502–509; d) N. S. Lawrence, R. P. Deo, J. Wang, *Anal. Chem.* **2004**, *76*, 3735–3739.
[7] a) T. You, O. Niwa, Z. Chen, K. Hayashi, M. Tomita, S. Hirono, *Anal. Chem.* **2003**, *75*, 5191–5196; b) Y. Sun, H. Buck, T. E. Mallouk, *Anal. Chem.* **2001**, *73*, 1599–1604; c) S. Park, T. D. Chung, H. C. Kim, *Anal. Chem.* **2003**, *75*, 3046–3049; d) E. Shoji, M. S. Freund, *J. Am. Chem. Soc.* **2001**, *123*, 3383–3384; e) J. Yuan, K. Wang, X. H. Xia, *Adv. Funct. Mater.* **2005**, *15*, 803–809; f) Y. Y. Song, D. Zhang, W. Gao, X. H. Xia, *Chem. Eur. J.* **2005**, *11*, 2177–2182.
[8] a) D. S. Bindra, G. S. Wilson, *Anal. Chem.* **1989**, *61*, 2566–2570; b) M. B. Jensen, D. C. Johnson, *Anal. Chem.* **1997**, *69*, 1776–1781; c) T. R. I. Cataldi, I. G. Casella, D. Centonze, *Anal. Chem.* **1997**, *69*, 4849–4855; d) W. R. LaCourse, D. C. Johnson, *Carbohydr. Res.* **1991**, *215*, 159–178.
[9] a) Yu. B. Vassilyev, O. A. Khazova, N. N. Nikolaeva, *J. Electroanal. Chem.* **1985**, *196*, 105–125; b) R. R. Adzic, M. W. Hsiao, E. B. Yeager, *J. Electroanal. Chem.* **1989**, *260*, 475–485.
[10] a) C.-J. Zhong, M. M. Maye, *Adv. Mater.* **2001**, *13*, 1507–1511; b) E. Granot, F. Patolsky, I. Willner, *J. Phys. Chem. B* **2004**, *108*, 5875–5881.
[11] a) J. Jia, B. Wang, A. Wu, G. Cheng, Z. Li, S. Dong, *Anal. Chem.* **2002**, *74*, 2217–2223; b) S. Tian, J. Liu, T. Zhu, W. Knoll, *Chem. Mater.* **2004**, *16*, 4103–4108.
[12] a) M. Zayats, R. Baron, I. Popov, I. Willner, *Nano Lett.* **2005**, *5*, 21–25; b) Y. Xiao, V. Pavlov, S. Levine, T. Niazov, G. Markovitch, I. Willner, *Angew. Chem. Int. Ed.* **2004**, *43*, 4519–4522; c) A. N. Shipway, E. Katz, I. Willner, *ChemPhysChem* **2000**, *1*, 18–52; d) Y. Xiao, F. Patolsky, E. Katz, J. F. Hainfeld, I. Willner, *Science* **2003**, *299*, 1877–1881.
[13] M. Valden, X. Lai, D. W. Goodman, *Science* **1998**, *281*, 1647–1650.
[14] a) M. Haruta, M. Daté, *Appl. Catal. A* **2001**, *222*, 427–537; b) M. M. Maye, Y. Lou, C.-J. Zhong, *Langmuir* **2000**, *16*, 7520–7523; c) Y. Lou, M. M. Maye, L. Han, J. Luo, C.-J. Zhong, *Chem. Commun.* **2001**, 473–474.
[15] M. S. El-Deab, T. Okajima, T. Ohsaka, *J. Electrochem. Soc.* **2003**, *150*, A851–A857.
[16] a) C. J. Brinker, G. W. Scherer, *Sol–Gel Science*, Academic Press, New York, **1990**; b) L. L. Hench, J. K. West, *Chem. Rev.* **1990**, *90*, 33–72.
[17] a) D. Avnir, *Acc. Chem. Res.* **1995**, *28*, 328–334; b) B. C. Dave, B. Dunn, J. S. Valentine, J. I. Zink, *Anal. Chem.* **1994**, *66*, 1120A–1127A.
[18] a) J. Wang, P. V. A. Pamidi, D. R. Zanette, *J. Am. Chem. Soc.* **1998**, *120*, 5852–5853; b) S. Bharathi, M. Nogami, S. Ikeda, *Langmuir* **2001**, *17*, 1–4.
[19] a) C. R. Raj, T. Okajima, T. Ohsaka, *J. Electroanal. Chem.* **2003**, *543*, 127–133; b) C. R. Raj, B. K. Jena, *Chem. Commun.* **2005**, 2005–2007; c) C. R. Raj, S. Behera, *Biosens. Bioelectron.* **2005**, *21*, 949–956.
[20] B. D. Cullity, *Elements of X-ray Diffraction*, Addison—Wesley, Reading, MA, **1978**, p. 102.
[21] K. R. Brown, D. G. Walter, M. J. Natan, *Chem. Mater.* **2000**, *12*, 306–313.
[22] a) M. W. Hsiao, R. R. Adzic, E. B. Yeager, *J. Electrochem. Soc.* **1996**, *143*, 759–767; b) L. D. Burke, P. F. Nugent, *Gold Bull.* **1998**, *31*, 39–50; c) L. A. Larew, D. C. Johnson, *J. Electroanal. Chem.* **1989**, *262*, 167–182; d) L. D. Burke, *Gold Bull.* **2004**, *37*, 125–135.
[23] K. R. Brown, M. J. Natan, *Langmuir* **1998**, *14*, 726–728.

Received: August 27, 2005
Revised: November 14, 2005
Published online: January 23, 2006

